Leak Detection in Pipelines Using the Damping of Fluid Transients

Xiao-Jian Wang[1], Martin F. Lambert[2], Angus R. Simpson[3], James A. Liggett[4*] and John P. Vítkovský[5]

Abstract: Leaks in pipelines contribute to damping of transient events. That fact leads to a method to find location and magnitude of leaks. Because the problem of transient flow in pipes is nearly linear, the solution of the governing equations can be expressed in terms of a Fourier series. All Fourier components are damped uniformly by steady pipe friction, but each component is damped differently in the presence of a leak. Thus, overall leak-induced damping can be divided into two parts. The magnitude of the damping indicates size of a leak whereas different damping ratios of the various Fourier components are used to find location of a leak. This method does not require rigorous determination and modeling of boundary conditions and transient behavior in the pipeline. The technique is successful in detecting, locating and quantifying a 0.1% size leak with respect to the cross-sectional area of a pipeline.

---

[1] Postgraduate Student, Dept. of Civil & Environmental Engineering, Adelaide University, Adelaide, SA 5005, Australia. email: xwang@civeng.adelaide.edu.au.

[2] Senior Lecturer, Dept. of Civil & Environmental Engineering, Adelaide University, Adelaide, SA 5005, Australia. email: mlambert@civeng.adelaide.edu.au.

[3] Associate Professor, Dept. of Civil & Environmental Engineering, Adelaide University, Adelaide, SA 5005, Australia. email: asimpson@civeng.adelaide.edu.au. Member, ASCE.

[4] Professor Emeritus, School of Civil & Environmental Engineering, Cornell University, Ithaca, N.Y. 14853-3501, USA. email: jal8@cornell.edu. *Corresponding author.

[5] Research Associate, Dept. of Civil & Environmental Engineering, Adelaide University, Adelaide, SA 5005, Australia. email: jvitkovs@civeng.adelaide.edu.au.

Introduction

Leakage from pipelines has the potential to cause significant environmental damage and economic loss. While pipelines are designed and constructed to maintain their integrity, it is difficult to avoid the occurrence of leakage in a pipeline system during its lifetime (Hovey and Farmer 1999). Often, accurate leak detection, enabling a quick response, is necessary to minimize damage. Leak detection methods previously proposed are: reflected wave or timing methods (Jönsson 1995, Covas and Romas 1999, Brunone 1999); volume balance methods (Griebenow and Mears 1989, Liou 1994); pressure or flow deviation methods (Griebenow and Mears 1989, Liou and Tian 1995); acoustic methods (Fuchs and Riehle 1991); pig-based monitoring and on-line surveillance methods (Black 1992, Weil et al. 1994, Furness and Reet 1998); frequency analysis methods (Jönsson and Larson 1992, Mpesha et al. 2001); inverse techniques (Pudar and Liggett 1992, Liggett and Chen 1994, Vítkovský, 2001); and a genetic algorithm method (Vítkovský et al. 2000). However, no single method can always meet operational needs from an accuracy and cost point of view (Furness and Reet 1998). Each of these leak detection techniques has its advantages and disadvantages in different circumstances. Liou (1998) used a pseudo-random binary signal (p.r.b.s) sequence as a transient tool and showed that change of the spatial damping of the p.r.b.s sequence along the pipeline can be used to detect a leak. A leak detection, location and quantification method that uses damping of a transient event by a leak is presented in this paper.

Transient response of a pipeline with a distributed leak was investigated by Wiggett (1968). They found that the transients in a pipeline were greatly affected by the magnitude of the distributed lateral flow. To investigate the effects of the demands on the transients in a field pipe network test, McInnis and Karney (1995) used a similar distributed leak

model based on the method of characteristics. Recent experimental and numerical work at Adelaide University has demonstrated that attenuation of transients in a pipeline due to a small leak is significant, as shown in Fig. 1. That observation has lead to this work, which attempts to detect leak occurrence, not by trying to model a transient event, as is required in inverse transient analysis (Liggett and Chen 1994), but by analyzing transient damping or decay of a pressure signal, a much simpler process. The technique does not require rigorous determination and modeling of boundary conditions and other transient behavior. It follows the approach used in pressure measurement where the (often large) common-mode pressure is removed through the use of differential rather than absolute pressure measurement devices. Baseline studies of pipelines that appear to be leak free can be used to increase the accuracy of the process, but are not necessary to apply the basic method. Transient pressure waves are used for the attenuation study because measurement of pressure in pipelines is more accurate (and considerably less expensive) than measurement of flow.

In the following section, the governing equations for unsteady pipeline flow with a leak are derived and non-dimensional parameters governing the behavior of pipeline transients are established. Analytical solutions for friction damping and leak damping are then obtained from the linearized equations. The leak detection method is developed in the next section followed by two numerical examples. Finally, results of experimental tests are presented.

Governing Equations

A control volume located between points 1 and 2 in Fig. 2 is used for the derivation of the unsteady flow equations (continuity and momentum) with leakage. The pipe is considered

to be horizontal with a leak located as shown in Fig. 2, where Q_L is the total discharge out of the leak located at $x = x_L$.

Adapting the non-leak equation of Wylie and Streeter (1993), conservation of mass in the control volume gives

$$\frac{\partial}{\partial t}(\rho A)\Delta x + \frac{\partial}{\partial x}(\rho A V)\Delta x = -\rho Q_L \tag{1}$$

where x = distance along the pipeline, t = time, ρ = fluid density, A = cross-sectional area of the pipe, and V = velocity of flow. Dividing (1) throughout by Δx and letting Δx approach zero gives

$$\frac{\partial}{\partial t}(\rho A) + \frac{\partial}{\partial x}(\rho A V) = -\rho Q_L \delta(x - x_L) \tag{2}$$

The Dirac delta function is defined as

$$\delta(x - x_L) = \begin{cases} \infty & \text{if} \quad x = x_L \\ 0 & \text{otherwise} \end{cases}, \text{ and } \lim_{\varepsilon \to 0} \int_{x_L - \varepsilon}^{x_L + \varepsilon} \delta(x - x_L)\, dx = 1 \tag{3}$$

where ε = a small distance on the either side of the leak. Note that $\delta(x\text{-}x_L)$ has dimension of length^{-1}. Considering the compressibility of the water and the elasticity of the pipe wall with some simplifications (Wylie and Streeter 1993), Eq. (2) is expressed in the more usual water-hammer-equation form,

$$\frac{\partial H}{\partial t} + \frac{Q}{A}\frac{\partial H}{\partial x} + \frac{a^2}{gA}\frac{\partial Q}{\partial x} + \frac{a^2}{gA} Q_L \delta(x - x_L) = 0 \tag{4}$$

in which H = piezometric head, Q = flow rate in the pipeline, a = wave speed in the fluid, and g = gravitational acceleration. Similarly, conservation of momentum for a leak perpendicular to the pipe axis is

$$\frac{\partial H}{\partial x} + \frac{1}{gA}\frac{\partial Q}{\partial t} + \frac{Q}{gA^2}\frac{\partial Q}{\partial x} + \frac{fQ^2}{2DgA^2} - \frac{QQ_L\delta(x - x_L)}{gA^2} = 0 \tag{5}$$

where f = friction factor and D = pipe diameter. The last term in (5) is caused by the mass flow discontinuity at the leak in the pipeline. Eq. (5) assumes that pipe friction during a transient event is described by a constant steady-state Darcy-Weisbach friction factor, which is a common assumption. However, pipe friction during unsteady events can be significantly larger than that predicted by the Darcy-Weisbach equation. The effects of unsteady friction are considered later in the paper.

Leak discharge is a function of pressure in a pipe and size of a leak and is expressed by the orifice equation

$$Q_L = C_d A_L \sqrt{2g\Delta H_L} \tag{6}$$

where $\Delta H_L = H_L - z_L$ = pressure head at a leak (assuming pressure outside of the pipe is atmospheric), H_L = piezometric head in the pipeline at the leak, z_L = pipe elevation at the leak, C_d = leak discharge coefficient, and A_L = leak area. The following dimensionless quantities are used to non-dimensionalize (4), (5) and (6):

$$H^* = \frac{H}{H_1},\ t^* = \frac{t}{L/a},\ x^* = \frac{x}{L},\ Q^* = \frac{Q}{Q_0},\ \text{and}\ \delta(x^* - x_L^*) = \delta(x - x_L)L \tag{7}$$

in which H_1 = reference piezometric head (e.g., the head at a tank), L = pipe length, and Q_0 = reference flow rate. Substituting (6) and applying the dimensionless quantities in (7) to (4) and (5) gives

$$\frac{\partial H^*}{\partial t^*} + \frac{V_0}{a}\frac{Q^*\partial H^*}{\partial x^*} + \frac{aQ_0}{gAH_1}\frac{\partial Q^*}{\partial x^*} + \frac{aQ_0}{gAH_1}\frac{C_d A_L}{Q_0}\sqrt{2gH_1}\sqrt{\Delta H_L^*}\,\delta(x^* - x_L^*) = 0 \tag{8}$$

$$\frac{gAH_1}{Q_0 a}\frac{\partial H^*}{\partial x^*} + \frac{\partial Q^*}{\partial t^*} + \frac{V_0}{a}Q^*\frac{\partial Q^*}{\partial x^*} + \frac{fLQ_0}{2DAa}\left(Q^*\right)^2 - \frac{V_0}{a}\frac{C_d A_L\sqrt{2gH_1}}{Q_0}Q^*\sqrt{\Delta H_L^*}\,\delta\left(x^* - x_L^*\right) = 0 \tag{9}$$

Because V_0/a is normally small, the second term in (8) and the third and the last terms in (9) can be neglected. The dimensionless equations become

$$\frac{\partial H^*}{\partial t^*} + \frac{1}{F}\frac{\partial Q^*}{\partial x^*} + M\sqrt{\Delta H_L^*}\,\delta(x^* - x_L^*) = 0 \tag{10}$$

$$F\,\frac{\partial H^*}{\partial x^*} + \frac{\partial Q^*}{\partial t^*} + RQ^{*2} = 0 \tag{11}$$

where $R = \frac{fLQ_0}{2aDA}$, $M = \frac{C_d A_L}{A}\frac{2a}{\sqrt{2gH_1}}$, $F = \frac{H_1}{H_J}$ and $H_J = \frac{aV_0}{g}$ is the Joukowsky pressure head rise, resulting from an instantaneous reduction of velocity V_0 to zero. The dimensionless quantities R, M and F are used to characterize the leak problem.

Linearized Solutions

Expressing H^* and Q^* as steady-state values plus small transient quantities gives

$$H^* = H_0^* + h^*, \qquad Q^* = Q_0^* + q^* \tag{12}$$

where h^* = non-dimensional head deviation, H_0^* = non-dimensional steady head, q^* = non-dimensional flow deviation and Q_0^* = non-dimensional steady flow. When only linear terms are retained, the square root in (10) is expressed as

$$\begin{aligned}\sqrt{\Delta H_L^*} &= \sqrt{H_L^* - z_L^*} = \sqrt{H_{L0}^* + h^* - z_L^*} = \sqrt{\Delta H_{L0}^* + h^*} \\ &= (\sqrt{\Delta H_{L0}^*} + \frac{h^*}{2\sqrt{\Delta H_{L0}^*}})(1 + e_T)\end{aligned} \tag{13}$$

where $e_T = \dfrac{\sqrt{\Delta H_L^*} - (\sqrt{\Delta H_{L0}^*} + \dfrac{h^*}{2\sqrt{\Delta H_{L0}^*}})}{\sqrt{\Delta H_{L0}^*} + \dfrac{h^*}{2\sqrt{\Delta H_{L0}^*}}}$ is the truncation error in the Taylor expansion, ΔH_L^* = $H_L{}^*$-$z_L{}^*$ = dimensionless pressure head at the leak, $H_L{}^*$ = dimensionless piezometric head in the pipeline at the leak, $z_L{}^*$ = dimensionless elevation at the leak, and

H_{L0}^* = dimensionless steady-state piezometric head at the leak. Substituting (12) and (13) into (10) and (11) and neglecting e_T and $(q^*)^2$ terms yields

$$\frac{\partial h^*}{\partial t^*} + \frac{1}{F}\frac{\partial q^*}{\partial x^*} + M\frac{h^*}{2\sqrt{\Delta H_{L0}{}^*}}\delta(x^* - x_L^*) = 0 \tag{14}$$

$$F\frac{\partial h^*}{\partial x^*} + \frac{\partial q^*}{\partial t^*} + 2Rq^* = 0 \tag{15}$$

Applying the operation $\frac{\partial}{\partial t^*}[\text{Eq.(14)}] - \frac{\partial}{\partial x^*}\left[\frac{\text{Eq.(15)}}{F}\right]$ and using

$$\frac{1}{F}\frac{\partial q^*}{\partial x^*} = -\frac{\partial h^*}{\partial t^*} - M\frac{h^*}{2\sqrt{\Delta H_{L0}{}^*}}\delta(x^* - x_L^*) \tag{16}$$

from the continuity equation, Eq. (14), results in

$$\frac{\partial^2 h^*}{\partial x^{*2}} = \frac{\partial^2 h^*}{\partial t^{*2}} + \left[2R + M\frac{\delta(x^* - x_L^*)}{2\sqrt{\Delta H_{L0}{}^*}}\right]\frac{\partial h^*}{\partial t^*} - 2RM\frac{h^*\delta(x^* - x_L^*)}{2\sqrt{\Delta H_{L0}{}^*}} \tag{17}$$

Eq. (17) simplifies to

$$\frac{\partial^2 h^*}{\partial x^{*2}} = \frac{\partial^2 h^*}{\partial t^{*2}} + [2R + F_L\delta(x^* - x_L^*)]\frac{\partial h^*}{\partial t^*} - 2RF_L\delta(x^* - x_L^*)h^* \tag{18}$$

in which $F_L = \frac{M}{2\sqrt{\Delta H_{L0}^*}}$ is the leak parameter. Since $\Delta H_{L0}^* = \frac{H_{L0} - z_L}{H_1}$, if z_L= 0, the leak parameter is

$$F_L = \frac{\frac{C_d A_L}{A}\frac{2a}{\sqrt{2gH_1}}}{2\sqrt{\frac{H_{L0}}{H_1}}} = \frac{C_d A_L}{A}\frac{a}{\sqrt{2gH_{L0}}} \tag{19}$$

where H_{L0} = steady-state piezometric head at the leak.

Consider a pipeline connecting two reservoirs with constant water elevations. The boundary conditions are

$$h^*(0, t^*) = 0 \text{ and } h^*(1, t^*) = 0 \tag{20}$$

Alternatively, the problem of a pipeline connecting an upstream reservoir and a downstream valve can be considered by using a mirrored imaginary pipeline. The application of this technique is presented in the second numerical example later in the paper.

If a known transient is initiated in the pipeline, the initial conditions are given as

$$h^*(x^*,0) = f(x^*) \text{ and } \frac{\partial h^*(x^*,0)}{\partial t^*} = g(x^*) \tag{21}$$

in which $f(x^*)$ and $g(x^*)$ are known piecewise continuous functions in the range of $0 \le x^* \le 1$. The head variation in the pipeline is obtained by solving (18) subject to the boundary and initial conditions of (20) and (21). By applying a Fourier expansion, the solution to (18) is

$$h^*(x^*,t^*) = \sum_{n=1}^{\infty} \left\{ e^{-(R+R_{nL})t^*} \left[A_n \cos\sqrt{(n\pi)^2 - 4RR_{nL} - (R+R_{nL})^2}\, t^* \right.\right. \\ \left.\left. B_n \sin\sqrt{(n\pi)^2 - 4RR_{nL} - (R+R_{nL})^2}\, t^* \right] \sin(n\pi x^*) \right\} \tag{22}$$

in which $R_{nL} = F_L \sin^2(n\pi x_L^*)$

$$\text{or} \quad R_{nL} = \frac{C_d A_L}{A} \frac{a}{\sqrt{2gH_{L0}}} \sin^2(n\pi x_L^*) \quad (n = 1, 2, 3, \ldots) \tag{23}$$

R_{nL} is the leak-induced damping factor for component n, where x_L^* is the dimensionless location of the leak along the pipeline. Since values of R and R_{nL} are normally much smaller than unity, Eq. (22) is approximated as

$$h^*(x^*,t^*) = \sum_{n=1}^{\infty} \left\{ e^{-(R+R_{nL})t^*} \left[A_n \cos(n\pi t^*) + B_n \sin(n\pi t^*) \right] \sin(n\pi x^*) \right\} \tag{24}$$

The Fourier coefficients, A_n and B_n, are

$$A_n = 2\int_0^1 f(x^*) \sin(n\pi x^*) dx^* \qquad (n = 1, 2, 3, \ldots) \tag{25}$$

$$B_n = \frac{2}{n\pi}\int_0^1 g(x^*)\sin(n\pi x^*)dx^* + \frac{(R+R_{nL})A_n}{n\pi} \qquad (n = 1, 2, 3,...) \qquad (26)$$

Note that the friction damping coefficient, R (= $fLQ_0/2aDA$), of (24) does not depend on n provided f is constant. For this case, the Fourier components are damped exponentially by friction, and that damping for all components is equal. In fact, e^{-Rt^*} can be taken outside of the summation in (24). In contrast, the leak-induced damping factor, R_{nL} of (24), depends on n and is different for each component; it cannot be removed from the summation sign in (24). A separate analysis, not reported in this paper, found that leak damping is approximately exponential when applied to the entire transient. Eq. (24) indicates that leak damping is exactly exponential when applied to a distinct Fourier component.

Application to Leak Detection

The solution in (24) shows that any measured pipeline transient is the summation of a series of harmonic components that are each exponentially damped with damping rate $R+R_{nL}$ (n = 1, 2, 3,…). If unsteady friction effects are negligible, the friction damping factor, R, is a function of steady flow conditions only and, its value is known. Alternatively, the value can also be experimentally determined by measuring the damping rate of a transient in a leak-free pipeline. Therefore, for a measured pipeline transient, if the damping rate $R+R_{nL}$ for an individual component can be obtained, the leak-induced damping factor R_{nL} can be found by subtracting R from $R+R_{nL}$.

Two types of measurement data, space-domain data and time-domain data, can be used for calculation of the damping coefficient $R + R_{nL}$. Space-domain data are obtained by measuring the transient pressure head at a number of locations along the pipeline at a

single time (in (24) t^* = constant and $0< x^*< 1$). Time-domain data are obtained by measuring the transient pressure history at a single pipeline location (in (24) x^* = constant and $t^*> 0$). Since measurement of pressure history at a specific location is easier, time-domain data are used for calculation of damping rates. A separate study has shown that the damping rates of the harmonic components obtained using both space-domain data and time-domain data are identical. The feasibility of analyzing pipeline transient period by period is presented in Appendix B.

In (23) the leak-induced damping coefficient, R_{nL}, depends on leak size (C_dA_L), location of a leak (x_L^*) and component, n. An algorithm is developed in this section to locate a leak utilizing the different damping of separate harmonics and to quantify a leak using the magnitude of damping. The process of leak detection, location and quantification is as follows:

1. Set up steady flow in the pipeline and then introduce a transient event.
2. Measure the variation of pressure head with time at one or more points along the pipe.
3. Divide the pressure trace into separate periods (Period 1, Period 2, etc. as shown in Fig. B1 of Appendix B) so that each can be analyzed individually.
4. Using a Fourier transformation, such as the Discrete or Fast Fourier Transforms (Press et al. 1992), decompose one period of the transient into its separate harmonic components and calculate the amplitude of each component. The amplitude $E_n^{(i)}$ of the n^{th} harmonic for the i^{th} period is expressed as

$$E_n^{(i)} = E_n^{(1)} e^{-(R+R_{nL})(i-1)T^*} \tag{27}$$

where $E_n^{(1)} = \dfrac{e^{-(R+R_{nL})(t_0^*+T^*)} - e^{-(R+R_{nL})t_0^*}}{-(R+R_{nL})T^*} \sin(n\pi x^*)\sqrt{A_n^2 + B_n^2}$ = amplitude of n^{th} harmonic component at the first period, t_0^* = dimensionless starting time of the analysis and T^* = dimensionless period defined as $T^* = T/(L/a)$, in which T = natural period of the pipeline. For the reservoir-pipeline-reservoir problem $T^* = 2.0$, and for the reservoir-pipeline-valve problem, $T^* = 4.0$. Details of derivation of (27) are given in Appendix B.

5. Repeat step 4 period by period along the pressure trace.
6. For each component n, plot the amplitude $E_n^{(i)}$ expressed in (27) versus period in terms of L/a. Compute the damping coefficient $R + R_{nL}$ from the plotted data using an exponential fitting function in form of (27) where both initial amplitude $E_n^{(1)}$ and the damping coefficient $R+R_{nL}$ can be calculated.
7. Analyze the damping rates of the separate components to determine occurrence, location and magnitude of the leak.

Determining existence, location and size of a leak using damping rates of separate components is now considered in detail.

Presence of a Leak

For a pipeline without a leak, $C_d A_L = 0$ in (23) and hence $R_{nL} = 0$; damping of each component is independent of component number, n, and is only dependent on friction damping factor, R. Therefore, given the same steady flow conditions followed by a transient event, presence of a leak is indicated by:

a. the damping rates $R+R_{nL}$ of the decomposed harmonic components, determined in step 6, are significantly different from each other, and

b. the damping rates for some components are larger than the friction-damping factor R.

Leak-induced damping depends strongly on the position of a leak and on n through a sine squared function in (23). Different components have different responses to a leak. For example, for a leak located in the middle of a pipeline ($x_L^* = 0.5$), components $n = 1$ and 3 have the maximum response whereas the response of component $n = 2$ is zero. Therefore, in practice more than one harmonic component should be used to detect a leak. Fig. 3 shows the relative response of the first three harmonics (n = 1, 2 and 3) to the different leak locations along the pipeline.

Location of a Leak

Applying a Fourier transform to a measured pipeline transient, leak location is calculated from the ratios of the different damping rates of a pair of harmonic components. Consider $n = n_1$ and $n = n_2$, for which leak damping factors are

$$R_{n_1 L} = \frac{C_d A_L a}{A\sqrt{2gH_{L0}}} \sin^2(n_1 \pi x_L^*) \text{ and } R_{n_2 L} = \frac{C_d A_L a}{A\sqrt{2gH_{L0}}} \sin^2(n_2 \pi x_L^*) \tag{28}$$

The ratio of these two terms is

$$\frac{R_{n_2 L}}{R_{n_1 L}} = \frac{\sin^2(n_2 \pi x_L^*)}{\sin^2(n_1 \pi x_L^*)} \tag{29}$$

which is a function of only leak location x_L^* and not a function of the leak size $C_d A_L$.

For a measured pipeline transient, the damping rate $R+R_{nL}$ for each harmonic component n can be calculated from its amplitude $E_n^{(i)}$ by analyzing each period. Since friction damping factor can be calculated from steady flow conditions, which are normally known, leak-induced damping $R_{n\mathrm{L}}$ for any component n is easily obtained by subtraction, giving the ratio of any two leak-induced damping rates as in (29). Solution of (29) for x_L^* yields

leak location. Fig. 4 is a plot of the theoretical relationship between the damping ratios of harmonic components $n_2 = 2$, $n_1 = 1$ and harmonic components $n_2 = 3$, $n_1 = 1$ with the corresponding leak locations in a pipeline.

Due to the symmetric nature of the sine squared function, the relationship between the damping ratio of two harmonic components and leak location is not unique. Two leak locations correspond to one value of the damping ratio R_{2L}/R_{1L} except for $x_L^* = 0.5$. For damping ratios of higher harmonic components, one damping ratio may correspond to a greater number of possible leak locations. For example, a damping ratio of $R_{3L}/R_{1L} < 1.0$ corresponds to four possible leak locations. Therefore, only harmonic components of $n = 1, 2, 3$ are used for leak detection analysis in this study.

Size of a Leak

Once the position of a leak has been determined, the magnitude of a leak can be easily calculated using (28). It is

$$C_d A_L = \frac{R_{nL} A \sqrt{2gH_{L0}}}{a \sin^2(n\pi x_L^*)} \qquad (n = 1, 2, 3, \ldots) \qquad (30)$$

where n is any one of the components. Theoretically, leak magnitude calculated using different components should be the same. Different measurement positions and different forms of transients can be used for added confirmation and to increase accuracy if necessary.

Sensitivity analysis

In the initial derivation, q^{*2} was neglected and the orifice equation was linearized in (13) in arriving at the (14) and (15). Reconsidering the equations without linearization gives

$$\frac{\partial^2 h^*}{\partial x^{*2}} = \frac{\partial^2 h^*}{\partial t^{*2}} + [2R' + F_L^{'}\delta(x^* - x_L^*)]\frac{\partial h^*}{\partial t^*} + 2R'F_L^{'}h^*\delta(x^* - x_L^*) + E\delta(x^* - x_L^*)] \qquad (31)$$

where $F_L^{'} = F_L(1+e_T)$, $R' = R(1+q^*)$, and $E = 2e_T R' M\sqrt{H_{L0}^*}$. Assuming a constant q^*, an approximate solution for (31) is

$$h^*(x^*, t^*) = \sum_{n=1}^{\infty}\left\{e^{-(R'+R_{nL}^{'})t^*}\left[A_n\cos(n\pi t^*) + B_n\sin(n\pi t^*)\right]\sin(n\pi x^*)\right\} \qquad (32)$$

in which $R_{nL}^{'} = F_L^{'}\sin^2(n\pi x_L^*) = (1+e_T)R_{nL}$. From (32), leak damping is only influenced by the value of e_T, which is the linearization error of the orifice equation. Neglecting q^{*2} has no direct influence on the location and quantification of a leak. Noticing that the ratio of any two leak damping coefficients of R'_{nL} is independent of parameter e_T, then the location of a leak is not affected by the error in the linearization of orifice equation. The error of leak size induced by the orifice linearization is defined as

$$\varepsilon_s = \frac{(C_d A_L)_{real} - (C_d A_L)_{apparent}}{(C_d A_L)_{real}} \qquad (33)$$

Substituting (30) into (33) gives

$$\varepsilon_s = \frac{R_{nL} - (1+e_T)R_{nL}}{R_{nL}} = -e_T = -\frac{\sqrt{1+h^*/H_{L0}^*} - (1+0.5h^*/H_{L0}^*)}{\sqrt{1+h^*/H_{L0}^*}} \qquad (34)$$

Variation of relative leak size error with parameter of h^*/H_{L0}^* is plotted in Fig. 5. To avoid negative pressure in a pipeline, h^*/H_{L0}^* must be less than 1.0. Within this range, the error in the size of a leak caused by the orifice linearization is less than 6% and thus not significant.

Neglecting the q^{*2} term has no direct influence on location and quantification of a leak, but it does affect friction damping. Because leak damping may be obtained by measuring total damping and subtracting friction damping, linearization may indirectly lead to an

experimental error in leak damping. That error shows up in the ratio of the Fourier components and thus influences the calculation of leak location.

By including the term of q^{*2}, the total damping is $R_{nL} + R(1+q^*)$. If leak damping is obtained by subtracting friction damping R that is calculated from the steady state, the calculated leak damping coefficient is $R_{nL} + Rq^*$, in which R_{nL} is the real leak damping. Then the ratio of leak damping of any two Fourier components is

$$\frac{R_{n_2L} + q^* R}{R_{n_1L} + q^* R} = \frac{\sin^2[n_2\pi(x_L^* + \varepsilon_L)]}{\sin^2[n_1\pi(x_L^* + \varepsilon_L)]} \tag{35}$$

in which ε_L = dimensionless distance away from a real leak location. Substituting $\frac{R_{n_2L}}{R_{n_1L}} = \frac{\sin^2(n_2\pi x_L^*)}{\sin^2(n_1\pi x_L^*)}$ into (35) and rearranging gives

$$\frac{\frac{\sin^2(n_2\pi x_L^*)}{\sin^2(n_1\pi x_L^*)} + T}{1+T} = \frac{\sin^2[n_2\pi(x_L^* + \varepsilon_L)]}{\sin^2[n_1\pi(x_L^* + \varepsilon_L)]} \tag{36}$$

where $T = \frac{Rq^*}{R_{n_1L}}$. The leak location error, ε_L, is a function of parameter T and real leak location, x_L^*. Variation of ε_L with parameter T and leak location x_L^* is presented in Fig. 6 if the first two Fourier components, $n_1 = 1$ and $n_2 = 2$, are used. Due to symmetry, only half of the pipeline is plotted. Fig. 6 indicates that large values of parameter T cause large errors in the location of leak, and leaks at different locations have different sensitivities to the parameter T. Leaks close to $x_L^* = 0.33$ are least influenced by error in the friction damping when the first two harmonics are used.

Leak size error, assuming that pressure at the leak is little influenced by leak location error, gives

$$\varepsilon_s = \frac{(C_d A_L)_{real} - (C_d A_L)_{apprarent}}{(C_d A_L)_{real}} = 1 - \frac{(1+T)\sin^2(n\pi x_L^*)}{\sin^2[n\pi(x_L^* + \varepsilon_L)]} \tag{37}$$

Variation of relative leak size error ε_s with parameter T and leak location x_L^* is presented in Fig. 7. Since leaks close to the ends of the pipeline cause less damping, a small error in the value of leak damping can cause a large error in the calculation of the leak size despite small T. In the application of the proposed leak detection method, small values of parameter T can be achieved by using small magnitudes of pipeline transient or small values of friction damping. The latter is achieved by using a low steady–state flow rate in the pipeline. Alternatively, friction damping can be obtained from a test in a leak-free pipeline or calculated using a numerical model. An example for such a situation is given in the second numerical application later in the paper.

Unsteady Friction Damping

In the derivation of (5), friction loss was assumed to be represented by a steady-state friction relationship. For rapidly varying flow, experiments have shown that damping of transients is greater than that predicted by the Darcy-Weisbach head loss equation. This difference can be addressed using unsteady friction models such as those by Zielke (1968), Brunone et al. (1991), Vardy and Hwang (1991), and Bergant et al. (2001). Applying an unsteady friction model, the total friction factor f is expressed as

$$f = f_s + f_u \tag{38}$$

where f_s represents the quasi-steady contribution and f_u is an additional contribution due to unsteadiness. To account for the unsteady friction damping, the friction-damping factor R in (24) is replaced by

$$R = R_s + R_u \tag{39}$$

in which R_s represents damping by steady friction, and R_u represents damping by unsteady friction. In contrast to steady friction damping, R_s, the value of unsteady friction damping, R_u, is not constant, and is different for different Fourier components. For this case, the e^{-Rt^*} term in (24) can not be taken outside the summation sign. The value of R_u (and hence R) can be determined by experimental tests or by a numerical model that incorporates an appropriate unsteady friction model, e.g. the modified Brunone model (Vitkovský, 2001).

Numerical Verification

The leak detection method discussed above is tested numerically in an artificial pipeline, shown in Fig. 8, using the results of simulated transients calculated from the method of characteristics (MOC). Two types of problems, a reservoir-pipeline-reservoir system and a reservoir-pipeline-valve system, are considered.

Reservoir-Pipeline-Reservoir Problem

In this case a transient in the pipeline is initiated by closing a side-discharge valve located 750m ($x^* = 0.75$) away from the upstream reservoir as shown in Fig. 8, while the valve adjoint to the downstream reservoir is fully open with negligible head loss. The magnitude of the side-discharge valve coefficient is $C_dA_S/A = 0.001$ where A_S = area of the side-discharge valve. Closing time of the valve is 0.05s. For the first test (case 1) the leak at $x_L^* = 0.25$ is removed ($C_dA_L/A = 0$) while for case 2 a leak of relative size of $C_dA_L/A = 0.001$ is assumed. The transient head in the pipeline is calculated numerically by a standard method-of-characteristics program using 16 pipe reaches. The calculations are started from steady state. The Darcy-Weisbach friction factor is calculated as $f = 0.015$ using the Swamee-Jain formula. The steady state friction-damping factor is $R = 0.0742$ (also R_s) with a steady-flow Reynolds number of 3.96×10^5. The sensitivity parameter, T,

is calculated as 0.0063. Based on previous sensitivity analysis, the leak location error, ε_L, and leak size error, ε_s, are both less than 1%.

Fig. 9 presents the leak detection analysis using the "measured" transient. Measured pressures at $x^* = 0.75$ are shown in Fig. 9(a) for cases of no leak (case 1) and with a leak (case 2). The amplitudes for separate components, n, are obtained by applying a discrete Fourier transform algorithm to analyze the measured data in Fig. 9(a), the results of which are presented in Fig. 9(b) for the first period signal ($t^* = 0.0 \sim 2.0$). The transient signals were analyzed period by period with an interval of $t^* = 2.0$. Fig. 9(c) shows computed amplitudes of the Fourier series of the first three harmonic components plotted against period in terms of L/a. In Fig. 9(c1)—the no leak case—the damping rate $R+R_{nL}$ for all three harmonic components is determined to be $R = 0.0742$ by fitting (27) to the decaying amplitudes. In Fig. 9(c2)—in which a leak was present—the damping rates $R+R_{nL}$ are 0.0991, 0.1232, 0.0992 for the first three components. The second value is significantly different from the first and third and all are larger than the friction-damping factor. The leak-induced damping rates R_{nL} for components $n = 1$, 2 and 3 are 0.0249, 0.0490 and 0.0250, which are obtained by subtracting R from $R+R_{nL}$ (see Table 1). The ratios of two leak-induced damping rates defined in (29) are $R_{2L}/R_{1L} = 1.97$ and $R_{3L}/R_{1L} = 1.00$. Using these two ratios in Fig. 4, corresponding leak locations are either $x_L^* = 0.25$ or $x_L^* = 0.75$, the former being the real leak location. Applying (30) based on either of the calculated leak locations and $R_{1L} = 0.0249$, the calculated leak size is $C_d A_L/A = 0.001$, which is identical to the real magnitude of the leak used to generate the MOC transient data.

Following the same procedure, transient damping, measured at different pipeline positions, $x^* = 0.375$, 0.5, and 0.625, was analyzed. Damping rates for separate harmonic

components are presented in Table 2. The Fourier transform analysis of transients measured at different locations give almost identical results for the damping rate for each component except for R_{2L} at $x^* = 0.5$, where a large error is introduced since the amplitude of the component $n = 2$ is close to zero.

The results in Table 2 for R_{1L} and R_{3L} show that the analysis can be performed for the measurement site located anywhere ($0<x^*<1$) along the pipeline. The results of the Fourier series analysis of numerical and experimental verifications presented in Figures 9, 12 and 13 are included in Table 1.

Reservoir-Pipeline-Valve Problem

A reservoir-pipeline-valve case provides an additional numerical example. For the pipeline of 1000m (between $x^* = 0.0$ and 1.0) in Fig. 10, a transient is initiated by closing the downstream valve. The initial steady flow in the pipeline is $Q_0 = 2.0$ L/s, which can be achieved by a partially opened downstream valve. The Reynolds number of the flow in pipeline is 11,160. The Darcy-Weisbach friction factor is calculated as $f = 0.0302$ using the Swamee-Jain formula and the friction damping factor $R_s = 0.0048$. The leak detection method presented earlier in the paper was developed from the general solution presented in (24) based on boundary conditions of two constant-head reservoirs. Thus, it cannot be directly applied to this particular example; however, it can be applied by adding an imaginary symmetric section (dashed portion) to the original pipeline as shown in Fig. 10.

Two cases, referred to as case 3 and case 4, are considered. In case 3, no leak is present in the pipeline, and in case 4, a leak of $C_dA_L/A = 0.001$ is present at $x^* = 0.25$. The transient pressures, generated by MOC for the original pipeline, are measured at $x^* = 0.75$ for the

two cases that are presented in Fig. 11(a). The presence of the leak has very obvious effects on the transient damping and shape. Note that the period of the transients is $4L/a$ for cases 3 and 4, while for cases 1 and 2 the transient period is $2L/a$.

The amplitudes of different harmonic components of the first period transient ($t^* = 0.0 \sim 4.0$) are given in Fig. 11(b) for cases 3 and 4 respectively. Amplitudes of all even harmonic components (n = 2, 4, 6,…) are close to zero. Damping of the first two odd harmonics, fitted using (27), are presented in Fig. 11(c). Due to the large magnitude of q^* ($q^* = 1.0$) in this case, sensitivity parameter T is calculated as 0.35. Therefore, as stated in the sensitivity analysis, the accuracy of leak detection will be significantly affected if the value used for friction damping is incorrect. As a result, the accurate value of the friction damping is obtained from a test in a leak-free pipeline (see case 3). For case 3, the friction damping rates determined from a leak-free pipeline are R = 0.0022 for harmonic components n = 1 and 3. For case 4, friction plus leak-induced damping rates for n = 1 and 3 are $R+R_{1L}$ = 0.0088 and $R+R_{3L}$ = 0.0410. Therefore, leak-induced damping for harmonic components n = 1 and 3 are R_{1L} = 0.0066 and R_{3L} = 0.0386 (see Table 1), and the damping ratio for the first and the third harmonics is R_{3L}/R_{1L} = 5.879. The corresponding leak positions are determined using Fig. 4 as $\hat{x}_1^* = 0.124$ or $\hat{x}_2^* = 0.876$. Applied to the real pipeline, the leak position of $\hat{x}_1^* = 0.124$ becomes $x^* = 0.248$, which is close to the real leak location of $x^* = 0.25$. The other possible leak is located in the imaginary symmetric section. As a result, the location detected using this type of transient system is unique. Applying $R_{1L} = 0.0066$ and $x_L^* = 0.124$ in (30), the magnitude of the leak is calculated as $C_dA_L/A = 0.0010$, which is identical to the actual leak size $C_dA_L/A = 0.001$.

Experimental Verification

Experimental tests were conducted in a single pipeline in the Robin Hydraulics Laboratory at Adelaide University. The pipeline is a straight 37.2m copper pipe with inner diameter of 22mm between two pressurized tanks as shown in Fig. 12. Five pressure transducers are located at equidistant points along the pipeline and two one-quarter-turn ball valves are installed at both ends for flow control. A side-discharge orifice, used to simulate a leak, is installed at the one-quarter position (point B) with exchangeable leak orifice sizes of 1mm, 1.5mm and 2mm diameter. To initiate a transient, another side-discharge valve is installed at point D. More details of this experimental apparatus are found in Vítkovský (2001).

Two tests were conducted. Test I is a no–leak case and in Test II a 1mm leak is located at point B (Fig. 12). The flow conditions are as follows: wave speed a = 1320m/s, head at tank 1 H_1 = 23.6m, head at Tank 2 H_2 = 22.8m and lumped leak parameter $C_d A_L$ = 5.00×10^{-7} m^2. The steady flow velocity in the pipeline is V_0 = 0.567m/s, and the steady friction damping factor is calculated as R_s = 0.0109.

In Test I, the valves at locations A and E and the side-discharge valve at D are opened and steady state achieved. The side-discharge valve at D is then closed quickly. In Test II, valves at locations A and E, the leak at B and the side-discharge valve at D are open until steady state is obtained. The side-discharge valve at D is then sharply closed. During the tests, pressure was measured by five pressure transducers at points A, B, C, D, and E. Only the measured pressures at point D (x^* = 0.75) for Test I and Test II are used for leak detection analysis and they are plotted in Fig. 13(a). The leak-induced damping of Test II is obvious compared to the transient in Test I that has no leak.

Fig. 13(b) shows the computed amplitudes of different harmonic components for the first period of the transient. The amplitude of each component is less in Test II than in Test I because the magnitude of the transient in test II is less than that in Test I due to the energy loss at the leak.

Friction damping factors obtained from the no-leak case (Test I) are presented in Fig. 13(c). Damping factors of the first three harmonic components (n = 1, 2, 3) are R_1 = 0.0244, R_2 = 0.0382, R_3 = 0.0563 (see Table 1), all being larger than the steady friction damping factor R_s = 0.0109, calculated using steady state friction. The differences between the measured and the calculated damping values are due to unsteady friction. It accounts for 50%, 71% and 80% of the total for the first three components. As a result, despite a small value of sensitivity parameter T (T = 0.00036), the friction damping in this case cannot be calculated from the steady state conditions, and must be obtained either from a leak-free measurement or from numerical analysis. As previously indicated, values of unsteady friction damping are different for different Fourier components. In Fig. 13(c), regression coefficients of the fitted curves of the damping factors are larger than 0.99, experimentally confirming the analysis that damping for each component is exponential.

In Tests I and II, since the steady flow conditions were similar and both the transients were initiated by closing the side-discharge valve at approximately the same speed, steady and unsteady friction effects are similar. Leak-induced damping rates for the first three harmonic components (n = 1, 2, 3) are R_{1L} = 0.0380, R_{2L} = 0.0798, R_{3L} = 0.0328 (see Table 1). The ratios of damping rates R_{2L} and R_{1L}, and R_{3L} and R_{1L} are $\frac{R_{2L}}{R_{1L}} = 2.10$, and

$\frac{R_{3L}}{R_{1L}} = 0.863$. Corresponding leak locations for these damping ratios are x_L^* = 0.242 (or x_L^* = 0.758) and x_L^* = 0.255 (or x_L^* = 0.745) by applying these two ratios in Fig. 4. Averaging of these results gives the location as x_L* = 0.249, almost the exact real location of the leak. Using R_{1L} = 0.0380, R_{2L} = 0.0801 and leak location x_L^* = 0.242 and x_L^* = 0.255, the magnitude of the leak is calculated, from (30), as $C_dA_L = 4.912\times10^{-7}$ and $C_dA_L = 4.917\times10^{-7}$ m^2, which are about 1.7% smaller than the real leak size of $C_dA_L = 5.00\times10^{-7}$ m^2.

Conclusions

Transients in pipelines are damped by both pipe friction and leaks. Steady state friction damping is independent of the harmonic component of the transient, but leak damping is different for different Fourier components. This fact can be used successfully to detect presence of leaks, to compute their location, and to find their size. The damping rate is useful for finding the quantity of leak discharge and the ratio of damping rates between different harmonic components is used to find leak location. Leaks of 0.1% of a pipeline's cross-sectional area or smaller can be detected and located.

A linearized analysis of the governing equations indicates that steady Darcy-Weisbach friction damping is exactly exponential, and leak damping is exponential for each of the individual harmonic components but only approximately exponential for an entire transient. Sensitivity analysis shows that linearization generates an insignificant error in both leak location and quantification. Inaccurate steady-state friction determination (if it is used to find the leak damping by subtraction from total damping), on the other hand, may or may not be significant, depending on the parameters of the pipeline and flow and

the location of a leak. Also, if subtraction is used to find leak damping, the added damping caused by unsteady flow may become important. Both nonlinear numerical analyses using the method of characteristics and laboratory experiments have verified the accuracy of the linearized solution in specific cases. The analysis of a linearized set of equations has provided significant insight into a leak detection technique.

Leak detection techniques based on analyzing pressure measurement during transient events in a pipe network have the obvious advantage of being orders of magnitude less expensive than field investigations. Although the leak detection technique presented in this paper does not have the generality of some other methods (e.g., the inverse transient method), and is not generally applicable to complex systems such as pipe networks, it is simple to use and apply.

Acknowledgements

The authors thank Prof. E. O. Tuck of the Department of Applied Mathematics, Adelaide University for the valuable discussion on the mathematical approach for the Dirac delta function. Financial support from the Australian Research Council to the second, third, and fourth authors and scholarships provided by the Australian Government and Adelaide University to the first author are gratefully acknowledged.

References

Abramowitz, M., and Stegun, I. A. (1972). *Handbook of Mathematical Functions with Formulas, Graphs, and Mathematical Tables*, National Bureau of Standards, Washington, USA.

Bergant, T., Simpson, A. R., and Vítkovský, J. (2001). "Developments in unsteady pipe friction modelling." *J. Hydr. Res.*, IAHR, 39(3), 249-257.

Black, P. (1992). "A review of pipeline leak detection technology." *Pipeline Systems*, B. Coulbeck and E. Evans eds., Kluwer Academic Publishers, 287-297.

Brunone, B., Golia, U. M., and Greco, M. (1991). "Modelling of fast transients by numerical methods." *Int. Meeting on Hydr. Transients with Column Separation,* IAHR, Valencia, Spain, 201-209.

Brunone, B. (1999). "Transient test-based technique for leak detection in outfall pipes," *J. Water Resour. Plng. and Mgmt.*, ASCE, Vol. 125, No. 5, 302-306.

Covas, D., and Romas, H. (1999). "Leakage detection in single pipeline using pressure wave behaviour." *Water Industry System: modelling and optimization application*, Baldock, Hertfordshire, England, 287-299.

Fuchs, H. V., and Riehle, R. (1991). "Ten years of experience with leak detection by acoustic signal analysis." *Applied Acoustics*, 33(1), 1-19.

Furness, R. A., and Reet, J. D. (1998). "Pipe line leak detection techniques*." Pipe Line Rules of Thumb Handbook*, E. W. McAllister, ed., Gulf Publishing Company, Houston, Texas, USA, 476-484.

Griebenow, G., and Mears, M. (1989). "Leak detection implementation: modeling and tuning methods." *J. Energ. Resour. Tech.,* ASME, 111, 66-71.

Hovey, D. J., and Farmer, E. J. (1999). "DOT states indicate need to refocus pipeline accident prevention." *Oil & Gas J.*, 97(11), 52-53.

Jönsson, L., and Larson, M. (1992). "Leak detection through hydraulic transient analysis." *Pipeline Systems*, B. Coulbeck and E. Evans, eds., Kluwer Academic Publishers, 273-286.

Liggett, J. A., and Chen, L.-C. (1994). "Inverse transient analysis in pipe networks." *J. Hydr. Engrg.,* ASCE, 120(8), 934-955.

Liou, C. P. (1994). "Mass imbalance error of waterhammer equations and leak detection." *J. Fluids Engrg.,* ASME, 116, 103-109.

Liou, C. P., and Tian, J. (1995). "Leak detection-transient flow simulation approaches." *J. Energ. Resour. Tech.,* ASME, 117, 243-248.

Liou, C. P. (1998). "Pipeline Leak Detection by Impulse Response Extraction." *J. Fluids Engrg.,* ASME, 120, 833-838.

McInnis, D., and Karney, B. (1995). "Transients in distribution networks: field tests and demand models." *J. Hydr. Engrg.,* ASCE, 121(3), 218-231.

Mpesha, W., Gassman, S. L., and Chaudhry, M. H. (2001). "Leak detection in pipes by frequency response method." *J. Hydr. Engrg.,* ASCE, 127(2), 134-147.

Press, W.H., Teukolsky, S.A., Vetterling, W.T., and Flannery, B.P. (1992). *Numerical Recipes: The Art of Scientific Computing*. Cambridge University Press, Cambridge, U.K.

Pudar, R. S., and Liggett, J. A. (1992). "Leaks in pipe networks." *J. Hydr. Engrg.,* ASCE, 118(7), 1031-1046.

Vardy, A. E., and Hwang, K.-L. (1991). "A characteristics model of transient friction in pipes." *J. Hydr. Res.,* IAHR, 29(5), 669-684.

Wiggert, D. C. (1968). "Unsteady flows in lines with distributed leakage." *J. Hydr. Div.,* ASCE, 94(HY1), 143-162

Vítkovský, J., Simpson, A. R., and Lambert, M. F. (2000). "Leak detection and calibration using transients and genetic algorithms." *J. Water Resour. Plng. and Mgmt.,* ASCE, 126(4), 262-265.

Vítkovský, J. (2001). "Inverse Analysis and Modelling of Unsteady Pipe Flow: Theory, Applications and Experimental Verification," Ph.D. Thesis, Department of Civil & Environmental Engineering, Adelaide University, Adelaide, Australia.

Weil, G. J., Graf, R. J., and Forister, L. M. (1994). "Remote sensing pipeline rehabilitation methodologies based upon the utilization of infrared thermography." *Proc*. of *Urban Drainage Rehabilitation Programs and Techniques,* ASCE, 173-181.

Wylie, E. B., and Streeter, S. L. (1993). *Fluid Transients in Systems*, Prentice-Hall Inc., Englewood Cliffs, N. J., USA.

Zielke, W. (1968). "Frequency-dependent friction in transient pipe flow." *J. Basic Engrg.,* ASME, 90, 109-115.

Appendix A: Notation

A = inner pipe cross-sectional area;

A_L = leak area;

A_S = area of side-discharge valve;

A_n, B_n = Fourier coefficients;

a = wave speed;

C = constant;

$C_0^{(i)}$ = Fourier coefficient of i^{th} period transient;

$C_m^{(i)}, D_m^{(i)}$ = Fourier coefficients of i^{th} period transient;

C_d = leak orifice discharge coefficient;

D = diameter of the pipe;

E = a parameter defined as $E = 2e_T R' M \sqrt{H_{L0}^*}$;

$E_n^{(1)}$ = amplitude of nth harmonic component of the first period transient;

$E_n^{(i)}$ = amplitude of nth harmonic component of the ith period transient;

e_T = truncation error in Taylor expansion;

F = a dimensionless head;

F_L, F_L' = leak parameter;

f = friction factor;

f_s = Darcy-Weisbach steady friction factor;

f_u = unsteady friction factor;

g = gravitational acceleration;

H = piezometric head;

H_0 = steady state piezometric head;

H_1 = a reference head in the pipeline;

H_J = Joukowsky head rise;

H_L = piezometric head at leak;

H_{L0} = steady piezometric head at leak;

H^* = dimensionless head $=H/H_1$;

$H_{L0}{}^*$ = dimensionless steady head at leak = H_{L0}/H_1;

h^* = dimensionless head disturbance;

L = length of pipeline;

M = leak parameter;

m, n = component number in a Fourier series;

P_n = n^{th} period of a transient;

p = pressure;

Q = flow rate;

Q_0 = steady state flow rate;

Q_L = flow rate through leak;

Q^* = dimensionless flow rate $=Q/Q_0$;

q^* = dimensionless flow rate disturbance;

R, R' = pipeline friction damping factor;

R_s = steady friction damping factor;

R_u = unsteady friction damping factor;

Re = Reynolds number;

$R_{nL}, R_{nL}^{'}$ = leak damping factor for n^{th} harmonic (n = 1,2,3,…);

T = natural period of pipeline; parameter used in sensitivity analysis;

T^* = dimensionless period of transient = $T/(L/a)$;

t = time;

t_0^* = dimensionless reference time;

t^* = dimensionless time = $t/(L/a)$;

V = flow velocity in the pipe;

V_0 = steady flow velocity in pipe;

x = distance along pipeline;

x^* = dimensionless distance = x/L;

x_L = position of leak;

x_L^* = dimensionless leak position = x_L/L;

$\hat{x}_1^*, \hat{x}_2^* ..$= dimensionless leak position in the combined real and imaginary pipeline;

ΔH_L = pressure head at the leak = H_L-z_L;

ΔH_L^* = dimensionless pressure head at the leak = H_L^*-z_L^*;

Δx = distance interval;

δ = Dirac delta function;

ε = roughness height for pipe wall; a small distance from the leak;

ε_L = dimensionless leak location error;

ε_S = dimensionless leak size error;

ρ = density of fluid;

Appendix B: Fourier analysis of the time-domain pressure variation data

When a time-domain transient (measured at a particular location x^*) is divided into sections period by period as shown in Fig. B1, each transient period can be expressed as a Fourier series based on (24).

For the first period P_1:

$$h^*(x^*,t^*)=\sum_{n=1}^{\infty}\left\{e^{-(R+R_{nL})t^*}\left[A_n\cos(n\pi t^*)+B_n\sin(n\pi t^*)\right]\sin(n\pi x^*)\right\}(t_0{}^*<t^*<t_0{}^*+T^*) \quad \text{(B1)}$$

where $t_0{}^*$ = starting time of analysis, and T^* = dimensionless period defined as T^* = $T/(L/a)$, in which T = natural period of pipeline. For the case in Fig. B1, T^* = 2.0.

For the second period P_2:

$$h^*(x^*,t_2^*)=\sum_{n=1}^{\infty}\left\{e^{-(R+R_{nL})t_2^*}\left[A_n\cos(n\pi t_2^*)+B_n\sin(n\pi t_2^*)\right]\sin(n\pi x^*)\right\} \qquad t_0^*+T^*<t_2^*<t_0^*+2T^* \quad \text{(B2)}$$

Setting $t_2^*=t^*+T^*$ and noticing the periodic property of the sinusoid functions give

$$h^*(x^*,t^*+T^*)=\sum_{n=1}^{\infty}e^{-(R+R_{nL})T^*}\left\{e^{-(R+R_{nL})t^*}\left[A_n\cos(n\pi t^*)+B_n\sin(n\pi t^*)\right]\sin(n\pi x^*)\right\} \qquad t_0^*<t^*<t_0^*+T^* \quad \text{(B3)}$$

For the i^{th} period P_i

$$h^*(x^*,t_i^*)=\sum_{n=1}^{\infty}\left\{e^{-(R+R_{nL})t_i^*}\left[A_n\cos(n\pi t_i^*)+B_n\sin(n\pi t_i^*)\right]\sin(n\pi x^*)\right\} \qquad t_0^*+(i-1)T^*<t_i^*<t_0^*+iT^* \quad \text{(B4)}$$

Setting $t_i^*=t^*+(i-1)T^*$ gives

$$h^*(x^*,t^*+(i-1)T^*)=\sum_{n=1}^{\infty}e^{-(R+R_{nL})(i-1)T^*}\left\{e^{-(R+R_{nL})t^*}\left[A_n\cos(n\pi t^*)+B_n\sin(n\pi t^*)\right]\sin(n\pi x^*)\right\} \qquad t_0^*<t^*<t_0^*+T^* \quad \text{(B5)}$$

A similar Fourier series is now fitted period by period to the "measured" transient data given in Fig. B1 (created by MOC). For the i^{th} period transient the fitted Fourier series is

$$h^*(x^*,t^*+(i-1)T^*) = C_0^{(i)} + \sum_{m=1}^{\infty}\left[C_m^{(i)}\cos(m\pi t^*) + D_m^{(i)}\sin(m\pi t^*)\right] \quad (t_0^* + < t^* < t_0^* + T^*) \quad \text{(B6)}$$

The Fourier coefficients $C_0^{(i)}$, $C_m^{(i)}$ and $D_m^{(i)}$ are defined as

$$C_0^{(i)} = \frac{1}{T^*}\int_{t_0^*}^{t_0^*+T^*} h^*(x^*,t^*+(i-1)T^*)dt^* \quad \text{(B7)}$$

$$C_m^{(i)} = \frac{2}{T^*}\int_{t_0^*}^{t_0^*+T^*} h^*(x^*,t^*+(i-1)T^*)\cos(m\pi t^*)dt^* \quad \text{(B8)}$$

$$D_m^{(i)} = \frac{2}{T^*}\int_{t_0^*}^{t_0^*+T^*} h^*(x^*,t^*+(i-1)T^*)\sin(m\pi t^*)dt^* \quad \text{(B9)}$$

Substituting the theoretical solution of $h^*(x^*, t^*+(i\text{-}1)T^*)$ from (B5) into (B7) gives

$$C_0^{(i)} = \frac{1}{T^*}\int_{t_0^*}^{t_0^*+T^*}\sum_{n=1}^{\infty} e^{-(R+R_{nL})(i-1)T^*}\left\{e^{-(R+R_{nL})t^*}\left[A_n\cos(n\pi t^*) + B_n\sin(n\pi t^*)\right]\sin(n\pi x^*)\right\}dt^* \quad \text{(B10)}$$

$$C_0^{(i)} = \frac{1}{T^*}\sum_{n=1}^{\infty}\sin(n\pi x^*)e^{-(R+R_{nL})(i-1)T^*}\int_{t_0^*}^{t_0^*+T^*}\left\{e^{-(R+R_{nL})t^*}\left[A_n\cos(n\pi t^*) + B_n\sin(n\pi t^*)\right]\right\}dt^* \quad \text{(B11)}$$

The integral term in (B11) is zero (Abramowitz and Stegun 1972). Therefore,

$$C_0^{(i)} = 0 \quad \text{(B12)}$$

Substituting the theoretical solution of $h^*(x^*, t^*)$ from (B5) into (B8) gives

$$C_m^{(i)} = \frac{2}{T^*}\int_{t_0^*}^{t_0^*+T^*}\sum_{n=1}^{\infty} e^{-(R+R_{nL})(i-1)T^*}\left\{e^{-(R+R_{nL})t^*}\left[A_n\cos(n\pi t^*) + B_n\sin(n\pi t^*)\right]\sin(n\pi x^*)\right\}\cos(m\pi t^*)dt^* \quad \text{(B13)}$$

$$C_m^{(i)} = \frac{2}{T^*}\sum_{n=1}^{\infty}\sin(n\pi x^*)e^{-(R+R_{nL})(i-1)T^*}\int_{t_0^*}^{t_0^*+T^*}\left\{e^{-(R+R_{nL})t^*}\left[A_n\cos(n\pi t^*) + B_n\sin(n\pi t^*)\right]\right\}\cos(m\pi t^*)dt^* \quad \text{(B14)}$$

The integral term in (B14) is zero except when $n = m$ (Abramowitz and Stegun 1972). Then (B14) is expressed as

$$C_n^{(i)} = \frac{e^{-(R+R_{nL})(t_0^*+T^*)} - e^{-(R+R_{nL})t_0^*}}{-(R+R_{nL})T^*} \sin(n\pi x^*) A_n e^{-(R+R_{nL})(i-1)T^*} \tag{B15}$$

Similarly by substituting (B5) into (B9) the Fourier coefficient $D_m^{(i)}$ is expressed as

$$D_n^{(i)} = \frac{e^{-(R+R_{nL})(t_0^*+T^*)} - e^{-(R+R_{nL})t_0^*}}{-(R+R_{nL})T^*} \sin(n\pi x^*) B_n e^{-(R+R_{nL})(i-1)T^*} \tag{B16}$$

The amplitude $E_n^{(i)}$ for a component n at the i^{th} period P_i is

$$E_n^{(i)} = \frac{e^{-(R+R_{nL})(t_0^*+T^*)} - e^{-(R+R_{nL})t_0^*}}{-(R+R_{nL})T^*} \sin(n\pi x^*) \sqrt{A_n^2 + B_n^2}\, e^{-(R+R_{nL})(i-1)T^*} \tag{B17}$$

or $$E_n^{(i)} = E_n^{(1)} e^{-(R+R_{nL})(i-1)T^*} \tag{B18}$$

where $E_n^{(1)} = \frac{e^{-(R+R_{nL})(t_0^*+T^*)} - e^{-(R+R_{nL})t_0^*}}{-(R+R_{nL})T^*} \sin(n\pi x^*) \sqrt{A_n^2 + B_n^2}$ is the amplitude of the component n at the first period.

Each Fourier component is exponentially damped in time. The damping rate of component n is $(R + R_{nL})$, which is the parameter to be determined.

Fig. 1. Damping caused by presence of a leak on the pipeline transients in a laboratory test.

Fig. 2. A pipe section with a leak

Fig. 3. Sensitivity of the leak position on the different harmonic components

Fig. 4. Damping ratios (Eq. (29)) of harmonic components

Fig. 5. Influence of linearization of orifice equation on the leak size

Fig. 6. Sensitivity of leak location on the sensitivity parameter T

Fig. 7. Sensitivity of leak size on the sensitivity parameter T

Fig. 8. A pipeline connected with two reservoirs

Fig. 9. Fourier series analysis of the transients measured from a pipeline without a leak (case 1) and with a leak (case 2) of $C_d A_L/A = 0.1\%$ at $x_L^* = 0.25$ ($T^* = 2.0$): (a) time history of the measured pipeline transients (MOC); (b) Fourier series analysis of the first period transient ($0 < t^* < 2.0$); and (c) damping of harmonic components with periods

Fig. 10. A pipeline connecting an upstream reservoir and downstream valve, and the added imaginary symmetric pipeline (D = 0.2m, a = 1000m/s, ε = 0.023mm).

Fig. 11. Fourier series analysis of the transients measured from a pipeline without a leak (case 3) and with a leak (case 4) of $C_d A_L/A$ = 0.1% at x_L^* = 0.25 by closing a downstream valve (T^* = 4.0): (a) time history of the measured pipeline transients (MOC); (b) Fourier series analysis of the first period transient ($0< t^* < 4.0$); and (c) damping of harmonic components with periods

Fig. 12. Experimental pipeline apparatus

Fig. 13. Experimental transients and Fourier series analysis results: (a) time history of the experimental transients; (b) Fourier series analysis results of the first period transient ($0< t^* < 2$); and (c) damping of harmonic components with periods (T^* = 2.0, and period number i =1, 2, 3,…)

Fig. B1. A time-domain pipeline transient (generated by MOC)

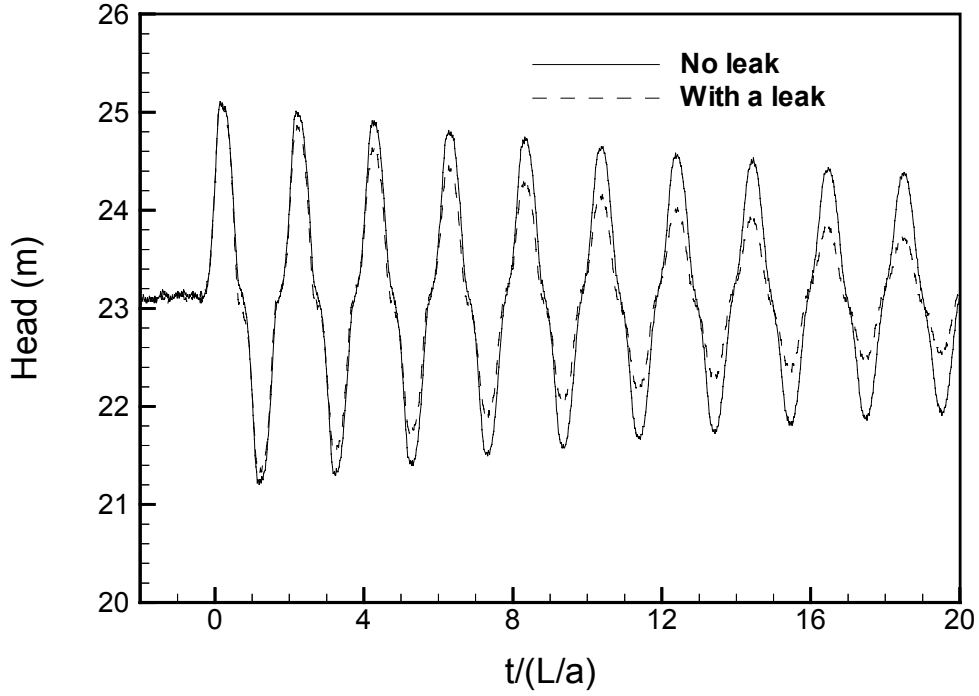
No leak
With a leak
Head (m)
t/(L/a)
26
25
24
23
22
21
20
0
4
8
12
16
20

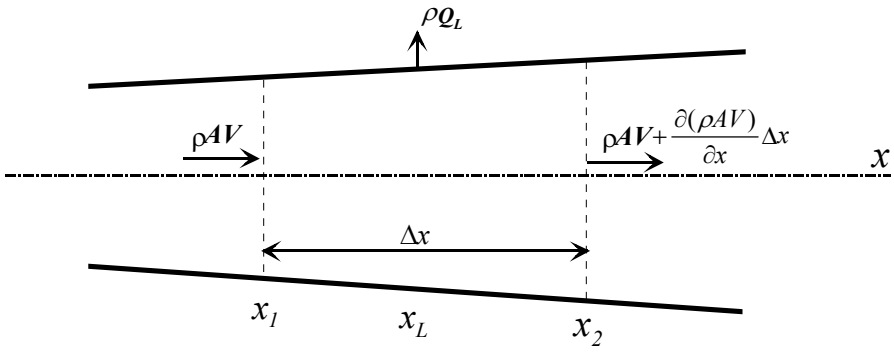
ρQ_L
ρAV
$\rho AV+\frac{\partial(\rho AV)}{\partial x}\Delta x$
x
Δx
x_1
x_L
x_2

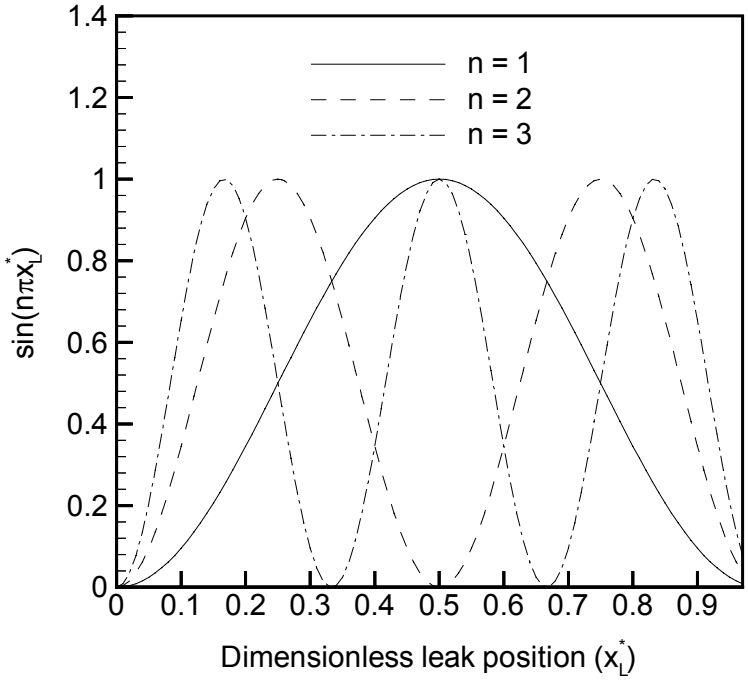
n = 1
n = 2
n = 3
1.4
1.2
1
0.8
0.6
0.4
0.2
0
0 0.1 0.2 0.3 0.4 0.5 0.6 0.7 0.8 0.9
sin(nπx*L)
Dimensionless leak position (x*L)

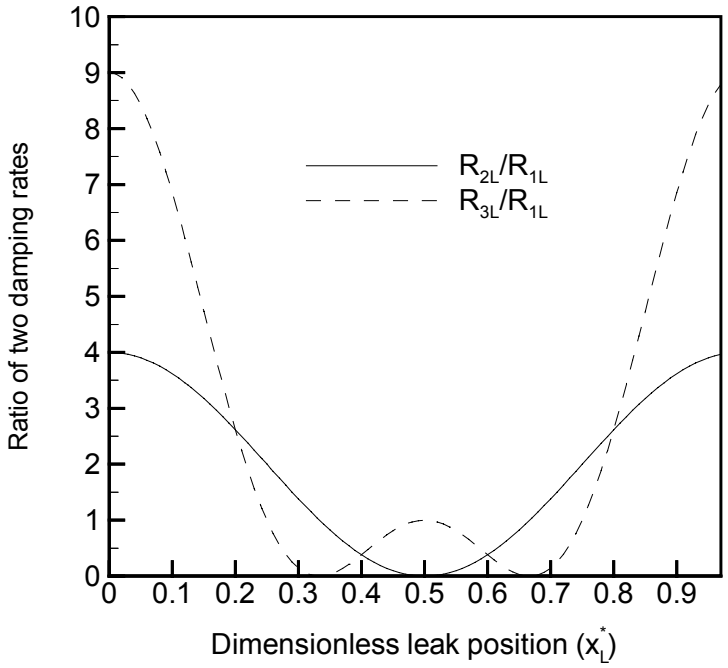
Ratio of two damping rates
Dimensionless leak position (x_L^*)
R_{2L}/R_{1L}
R_{3L}/R_{1L}
0
1
2
3
4
5
6
7
8
9
10
0
0.1
0.2
0.3
0.4
0.5
0.6
0.7
0.8
0.9

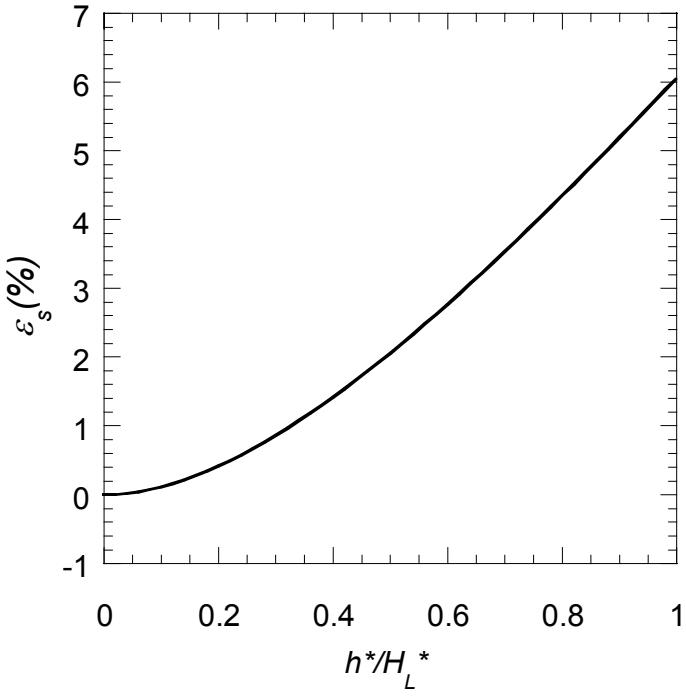
7
6
5
4
3
2
1
0
-1
ε_s(%)
0
0.2
0.4
0.6
0.8
1
h^*/H_L^*

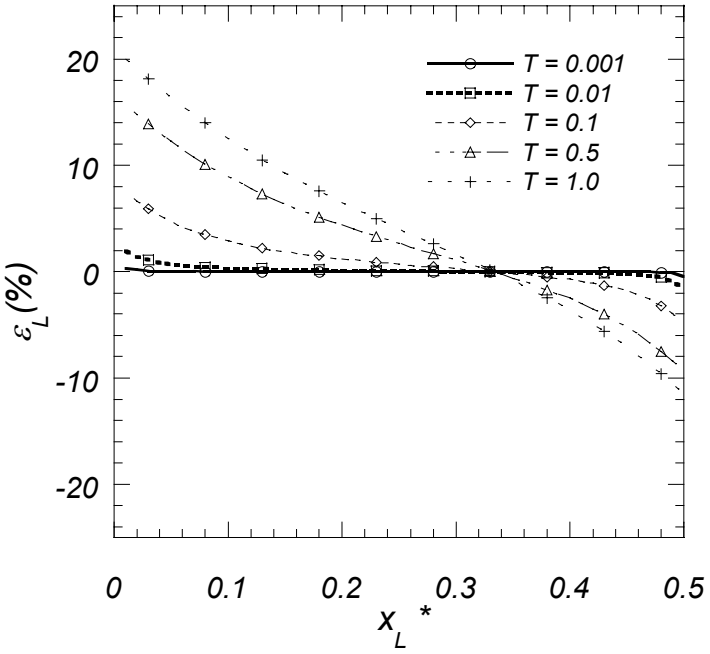
T = 0.001
T = 0.01
T = 0.1
T = 0.5
T = 1.0
20
10
0
-10
-20
ε_L (%)
0
0.1
0.2
0.3
0.4
0.5
x_L *

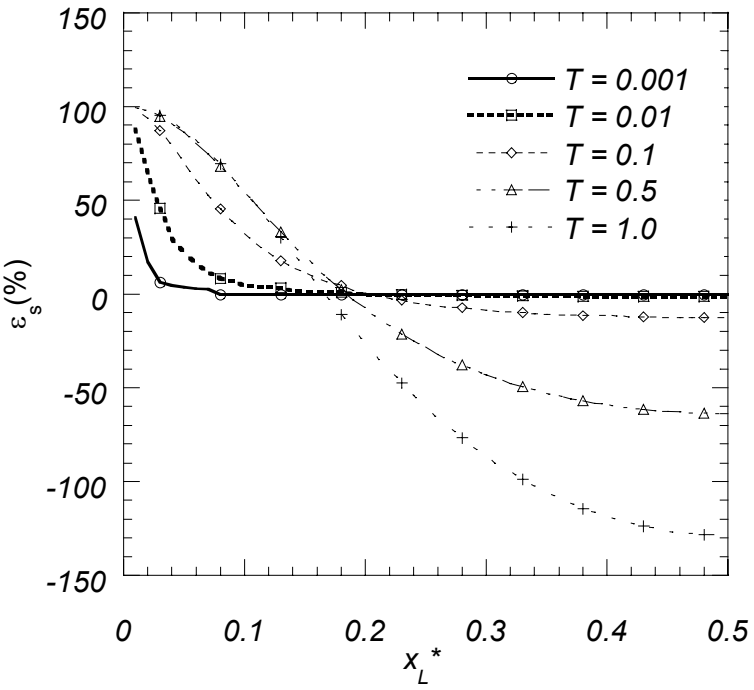
150
100
50
0
-50
-100
-150
0
0.1
0.2
0.3
0.4
0.5
x_L^*
ε_s (%)
T = 0.001
T = 0.01
T = 0.1
T = 0.5
T = 1.0

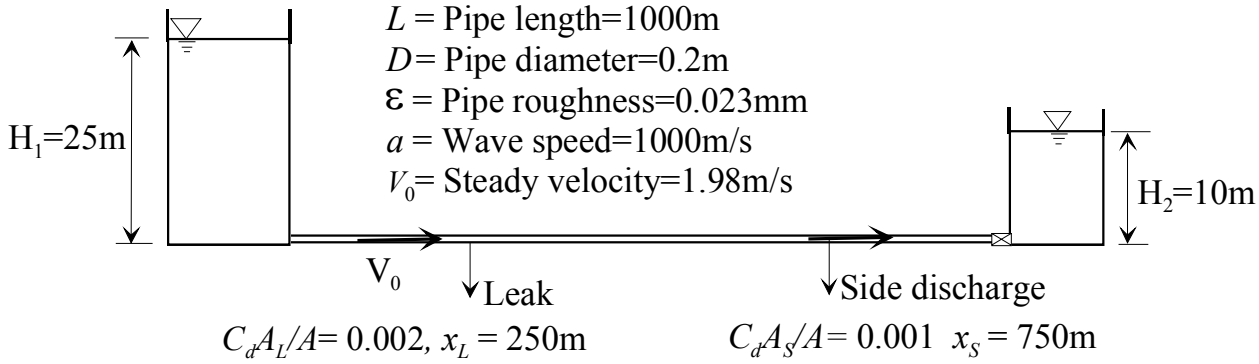
L = Pipe length=1000m
D= Pipe diameter=0.2m
ε = Pipe roughness=0.023mm
a = Wave speed=1000m/s
V_0= Steady velocity=1.98m/s
H_1=25m
H_2=10m
V_0
Leak
Side discharge
C_dA_L/A= 0.002, x_L = 250m
C_dA_S/A= 0.001 x_S = 750m

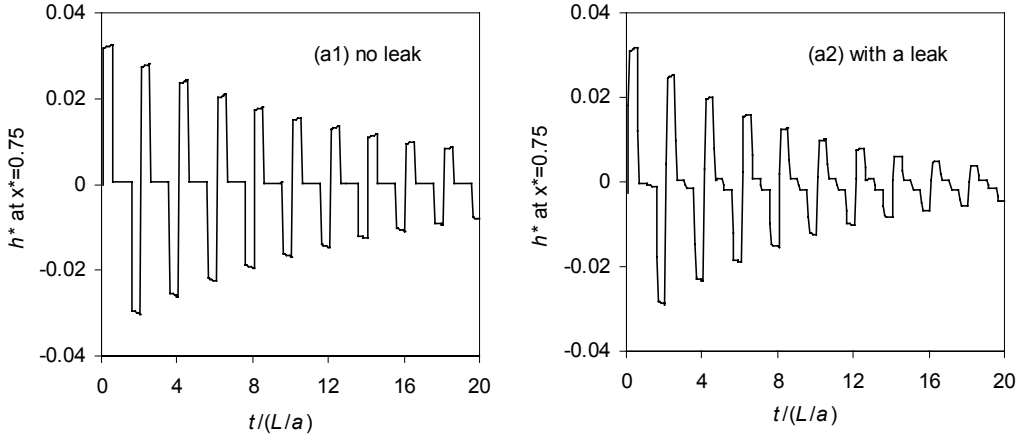
(a1) no leak
(a2) with a leak
h* at x*=0.75
t/(L/a)

(a)

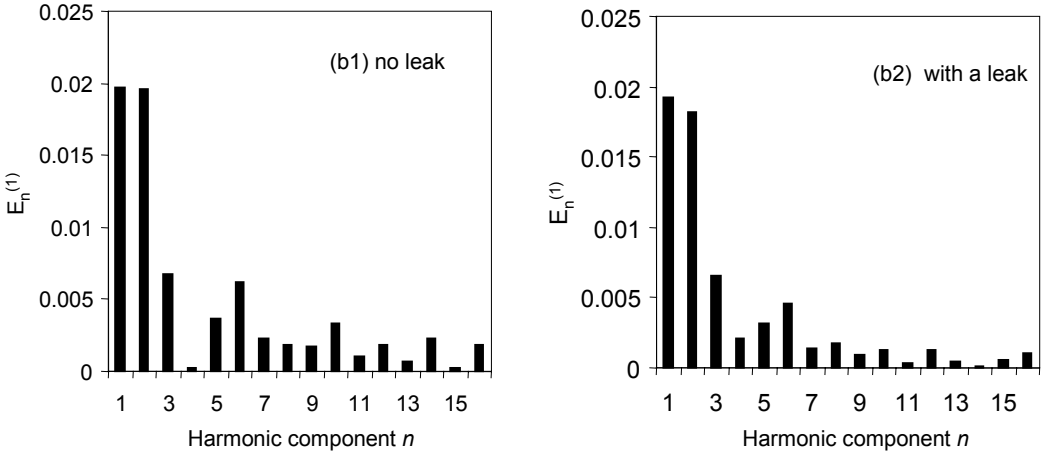
(b1) no leak
(b2) with a leak
E_n^(1)
Harmonic component n

(b)

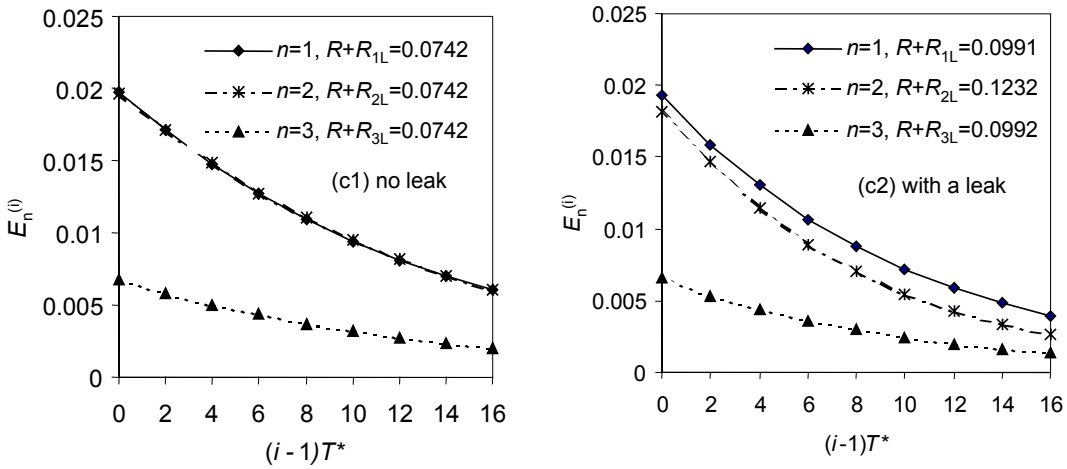
n=1, R+R1L=0.0742
n=2, R+R2L=0.0742
n=3, R+R3L=0.0742
(c1) no leak
n=1, R+R1L=0.0991
n=2, R+R2L=0.1232
n=3, R+R3L=0.0992
(c2) with a leak
E_n^(i)
(i-1)T*

(c)

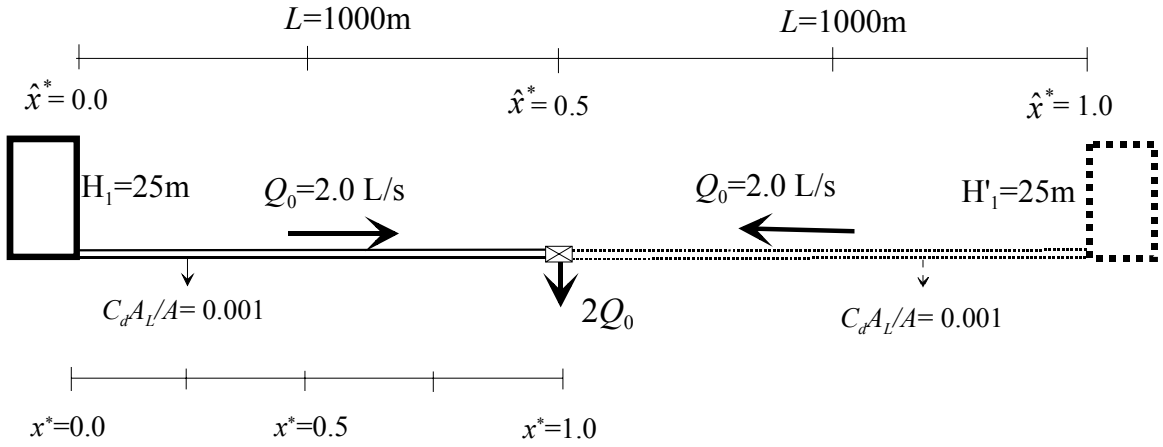
L=1000m
L=1000m
$\hat{x}^*$= 0.0
$\hat{x}^*$= 0.5
$\hat{x}^*$= 1.0
H1=25m
Q0=2.0 L/s
Q0=2.0 L/s
H'1=25m
CdAL/A= 0.001
2Q0
CdAL/A= 0.001
x*=0.0
x*=0.5
x*=1.0

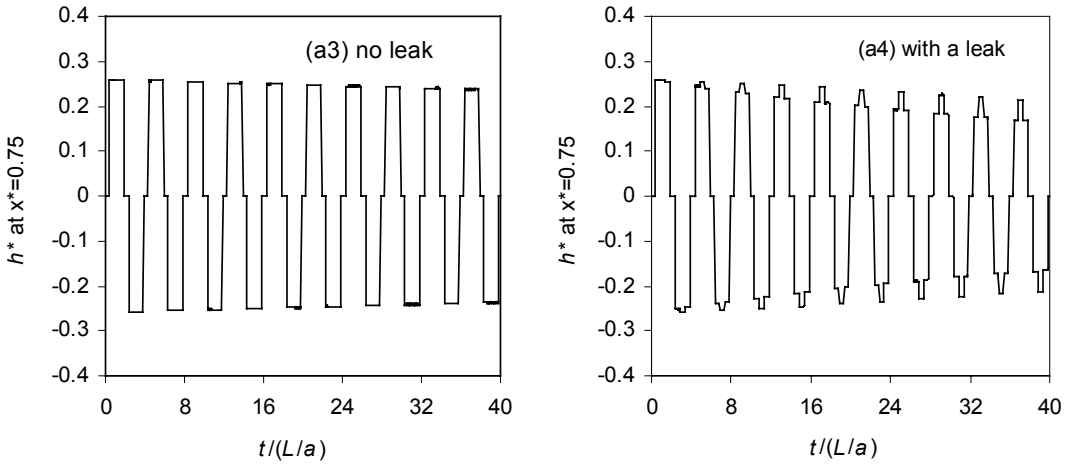
(a3) no leak
(a4) with a leak
h* at x*=0.75
t/(L/a)

(a)

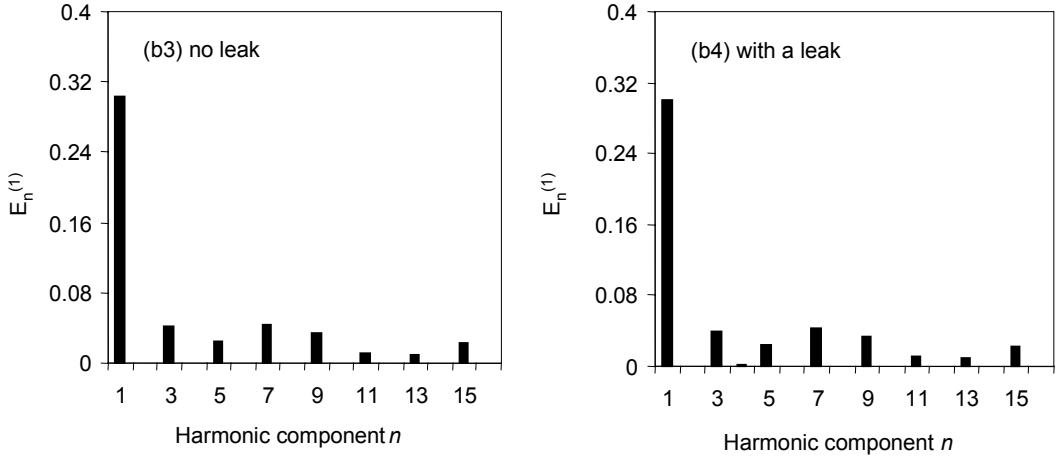
(b3) no leak
(b4) with a leak
E_n^(1)
Harmonic component n

(b)

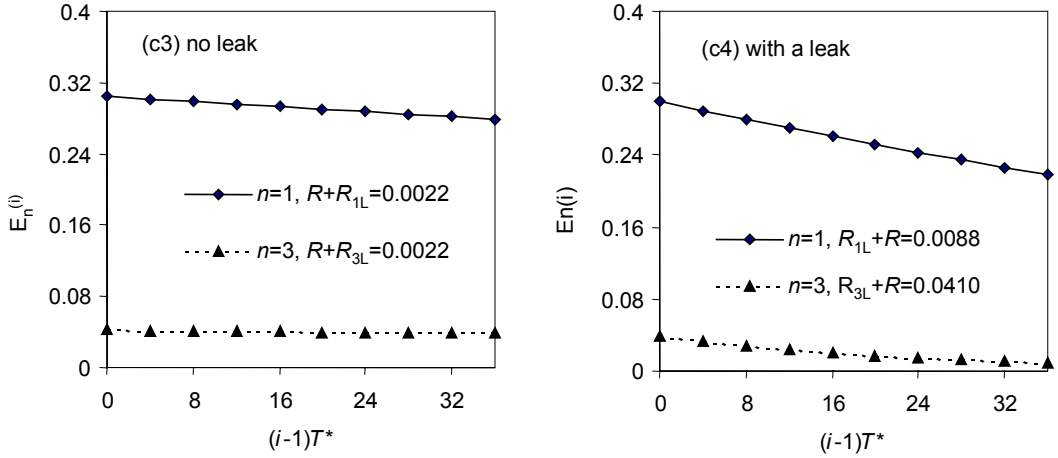
(c3) no leak
(c4) with a leak
n=1, R+R1L=0.0022
n=3, R+R3L=0.0022
n=1, R1L+R=0.0088
n=3, R3L+R=0.0410
E_n^(i)
En(i)
(i-1)T*

(c)

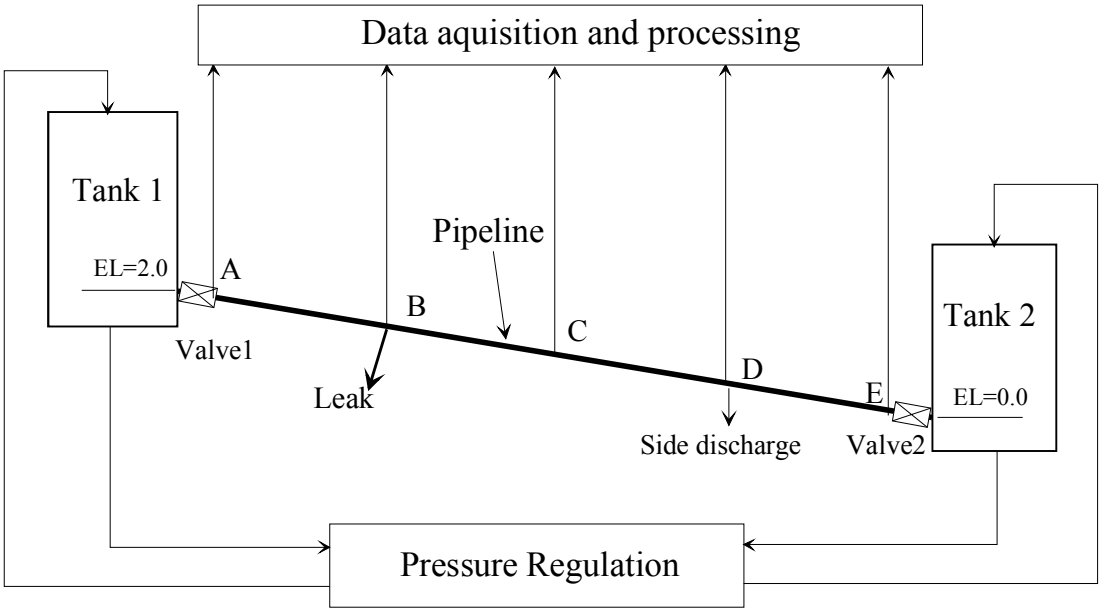
Data aquisition and processing
Tank 1
EL=2.0
A
Valve1
Pipeline
B
Leak
C
D
Side discharge
E
Valve2
Tank 2
EL=0.0
Pressure Regulation

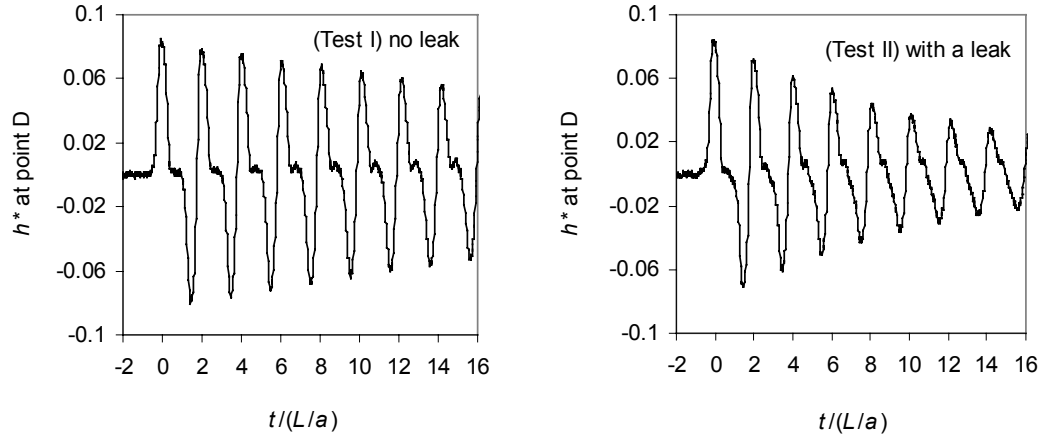
(Test I) no leak
(Test II) with a leak
h* at point D
t/(L/a)

(a)

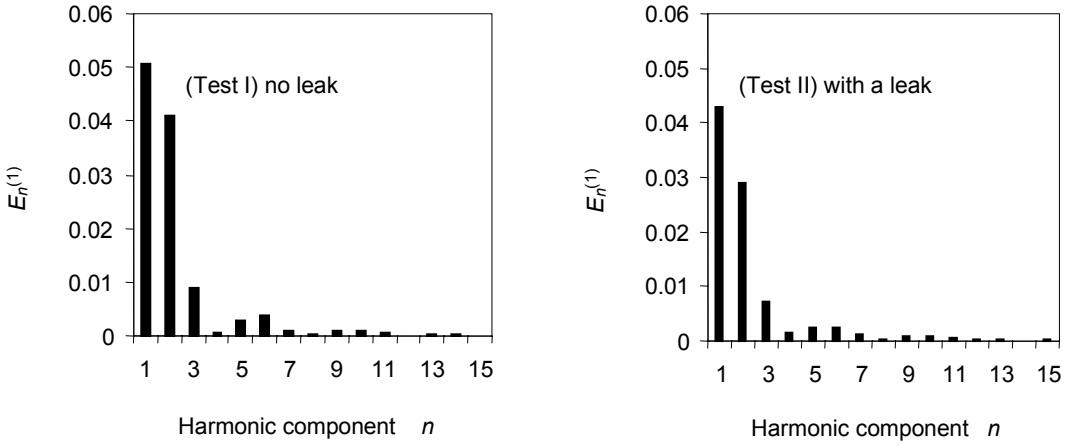
(Test I) no leak
(Test II) with a leak
Harmonic component n

(b)

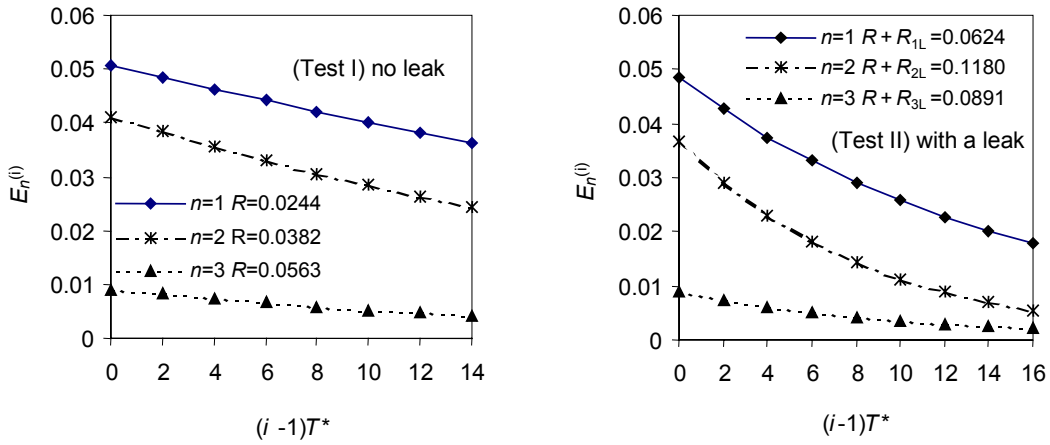
(Test I) no leak
n=1 R=0.0244
n=2 R=0.0382
n=3 R=0.0563
(Test II) with a leak
n=1 R + R1L =0.0624
n=2 R + R2L =0.1180
n=3 R + R3L =0.0891
(i -1)T*

(c)

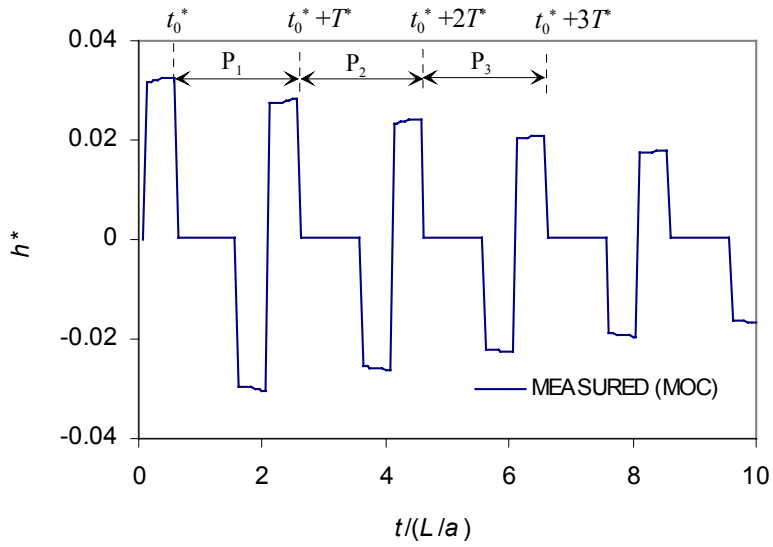
t_0^*
$t_0^* + T^*$
$t_0^* + 2T^*$
$t_0^* + 3T^*$
P1
P2
P3
0.04
0.02
0
-0.02
-0.04
h*
0
2
4
6
8
10
t/(L/a)
MEASURED (MOC)

Table 1. Results of Fourier transform analysis on the transients presented in numerical and experimental examples

Examples	**Cases**	**Harmonic Components**		
		***n* = 1**	***n* = 2**	***n* = 3**
Reservoir-Pipeline-Reservoir Problem (Fig. 9)	Case 1 (no leak) R	0.0742	0.0742	0.0742
	Case 2 (with a leak) $R+R_{nL}$	0.0991	0.1232	0.0992
	Leak damping R_{nL}	0.0249	0.0490	0.0250
Reservoir-Pipeline-Valve Problem (Fig. 11)	Case 3 (no leak) R	0.0022	N/A*	0.0022
	Case 4 (with a leak) $R+R_{nL}$	0.0088	N/A*	0.0410
	Leak damping R_{nL}	0.0066	N/A*	0.0388
Experimental Verification (Fig. 13)	Test I (no leak) R	0.0244	0.0382	0.0563
	Test II (with a leak) $R+R_{nL}$	0.0624	0.1180	0.0891
	Leak damping R_{nL}	0.0380	0.0798	0.0328

* The even harmonic components are equal to zero for the reservoir-pipeline-valve problem

Table 2. Results using transients from the different measurement locations (R = 0.0742)-Case 1

Measurement position	R_{1L}	R_{2L}	R_{3L}	R_{2L}/R_{1L}	R_{3L}/R_{1L}
$x^* = 0.375$	0.0248	0.0489	0.0249	1.972	1.004
$x^* = 0.5$	0.0247	0.0314	0.0247	1.271	1.000
$x^* = 0.625$	0.0248	0.0489	0.0251	1.972	1.012
$x^* = 0.75$	0.0249	0.0490	0.0250	1.968	1.004